



Yielding in multicomponent metallic glasses: Universal signatures of elastic modulus heterogeneities

Kamran Karimi ^{1,*}, Mikko J. Alava,^{1,2} and Stefanos Papanikolaou ^{1,†}¹NOMATEN Centre of Excellence, National Center for Nuclear Research, ulica A. Sołtana 7, 05-400 Swierk/Otwock, Poland²Aalto University, Department of Applied Physics, P.O. Box 11000, 00076 Aalto, Espoo, Finland

(Received 29 July 2022; accepted 26 April 2023; published 1 June 2023)

Sheared multicomponent bulk metallic glasses are characterized by both chemical and structural disorder that define their properties. We investigate the behavior of the local, microstructural elastic modulus across the plastic yielding transition in six Ni-based multicomponent glasses, that are characterized by compositional features commonly associated with solid solution formability. We find that elastic modulus fluctuations display consistent percolation characteristics pointing towards universal behavior across chemical compositions and overall yielding sharpness characteristics. Elastic heterogeneity grows upon shearing via the percolation of elastically soft clusters within an otherwise rigid amorphous matrix, confirming prior investigations in granular media and colloidal glasses. We find clear signatures of percolation transition with spanning clusters that are universally characterized by scale-free characteristics and critical scaling exponents. The spatial correlation length and mean cluster size tend to diverge prior to yielding, with associated critical exponents that exhibit fairly weak dependence on compositional variations as well as macroscopic stress-strain curve details.

DOI: [10.1103/PhysRevMaterials.7.063601](https://doi.org/10.1103/PhysRevMaterials.7.063601)

I. INTRODUCTION

In realistic studies of bulk metallic glasses, the associated yielding properties and shear banding behavior [1] have important industrial and technological implications in terms of the ductility of the glass. The ongoing eagerness to promote the latter (in combination with hardening properties) has already shifted the focus to the development of multicomponent glasses (also known as amorphous alloys and/or high-entropy metallic glasses) with a highly tunable microstructural/compositional complexity [2,3]. The atomistic origin of this new design paradigm is based on the common observation that glasses with a low atomic disparity limit (where the atomic radii of constituent elements are considered to be very similar) have a high capacity to form localized deformation patterns, whereas those at the opposite limit have a tendency to delocalize strain [4] and therefore deform in a more ductile way. In this context, the shear band structure and design-level ductility appear to be highly dependent on inherent heterogeneity as an essential elemental/compositional feature. However, the microstructural origins and elemental dependence of such inhomogeneities and, more importantly, the associated spatial-dynamical evolution upon shearing have yet to be explored.

Despite certain commonalities of failure properties across disordered solids [5], the sharpness of the yielding transition,

as a common signature of strain localization (and ductility), may show strong variations by altering thermal treatments and chemical compositions in bulk metallic glasses, ranging from uniformly distributed patterns to system-spanning crack-like features [2,4,6,7]. Owing to the presence of quenched chemical/structural disorder, glassy metals may accommodate a distributed plastic flow with a significant contribution to ductility [8–10]. Certain (aged) glasses that lack this heterogeneity element [11–13] (or associated lengths not exceeding interatomic scales) tend to localize strain within a single dominant band before shear instability results in a catastrophic brittle-type fracture.

In this context, tailoring elastic heterogeneity has recently emerged as a novel design framework to build more ductile metallic glasses [8,14]. Under special thermal treatments and variations of chemical elements, quenched metallic glasses may nucleate elastically soft clusters that become structured and span the entire system upon failure, leading to enhanced plastic flow and hence ductility. This is illustrated in Fig. 1 where the yielding transition, fine tuned by the chemical compositions, is accompanied by percolating networks of softness (shown in brown) in a driven CoNiFe and CoNiCrFe bulk metallic glass.

The relevance of percolation theory to mechanical stability and yielding transition has been a long-established notion [15–17]. The concept of percolation as a stability metric was implemented by Liu *et al.* in the context of marginally stable solids and jamming transitions [18–20]. Following a similar analogy in Ref. [21], Cates and Wyart proposed a mean-field approach accounting for the flow-induced percolation of frictional contacts that closely reproduced the phenomenology of discontinuous shear thickening in dense suspension flows. The percolation transition of softness and its relevance within the context of amorphous plasticity has been also established in (soft) model glasses [22–24] as well as colloidal systems [24,25] and model metallic glasses [26] under shear. Such

*kamran.karimi@ncbj.gov.pl

†Stefanos.Papanikolaou@ncbj.gov.pl

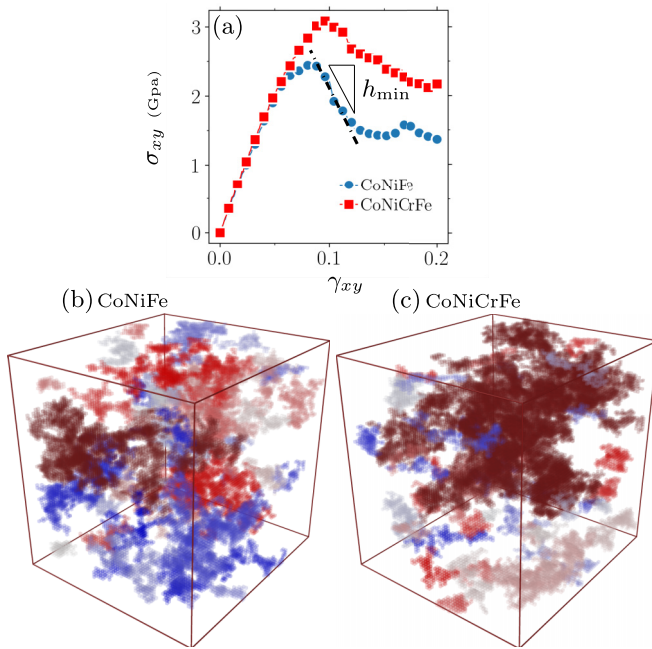


FIG. 1. Three-dimensional softness maps of the (b) CoNiFe and (c) CoNiCrFe compositions at applied shear strain $\gamma_{xy} \simeq 0.1$ and the corresponding stress-strain curves σ_{xy} vs γ_{xy} in (a). The colors in (b) and (c) indicate different clusters including elastically unstable regions with $\mu \leq 0$. The slope in (a) indicates the softening modulus h_{\min} . Upon shearing, negative- μ clusters form percolating networks (in brown) on approach to failure that tend to correlate with the (postfailure) macroscopic properties.

studies have mainly focused on certain (implicit) notions of softness based on the degree of deformation nonaffinity or shear-induced mobility that exhibit percolating features near the criticality. However, realistic studies of bulk metallic glasses driven out of equilibrium, with substantial industrial and technological implications, and associated composition dependence have been more challenging. In experimental studies of CuZr-based compositions [27,28], as a canonical metallic glass, the notion of a percolation transition was primarily used to interpret the marked growth in the measured plastic yield strain and hence ductility with the percolating ordered phase (as a result of alloying) within the amorphous matrix. Our motivation is somewhat similar: We show that yielding occurs through a percolation transition in metallic glasses but with chemical compositions that fine tune the former through percolating networks of softness.

Here, using atomistic simulations, we investigate six multicomponent bulk metallic glasses including Co, Ni, Fe, Cr, and Mn at compositions that have been the focus of recent experimental investigations. The chosen compositions are commonly believed to optimize solid solution formability, characterized by low misfit coefficients δ_a , and not thought to promote a glass-forming ability typically observed for $\delta_a > 6\%$ [29]. Nonetheless, there is a way to generate a glassy environment in the opposite limit of $\delta_a \rightarrow 0$ but maintaining a larger number of elements, as in medium/high entropy metallic glasses (see Ref. [3] and references therein).

By probing local elasticity, in particular shear modulus μ and its evolution toward failure, we present direct evidence

that plastic yielding in driven metallic glasses takes place universally through a percolation transition of softness, characterized by regions of negative $\mu \leq 0$ (as shown in Fig. 1). The sharpness of the yielding transition, fine tuned by chemical compositions and inferred from the rate of spontaneous drop h_{\min} in the stress response, exhibits consistent correlation features with softness and its percolation properties. Our cluster analysis associated with local elasticity maps features critical scaling properties, i.e., scale-free statistics, divergence of correlation lengths, and critical exponents that are reminiscent of a nonequilibrium phase transition.

From a broader perspective, our methodology offers a robust indicator of nonaffinity, e.g., the disorder-induced breakdown of a homogeneous response, by probing elastic heterogeneity in amorphous materials. Conceptually, our approach is similar to investigations of low-energy quasilocalized modes that are spatially distinguishable from long-wavelength phonon modes in elastic crystalline solids (see Ref. [30] and references therein). Predictive plasticity models solely based on the notion of shear transformation zones (STZs) might fail to capture such correlations because the latter are generally believed to be (micro)structural defects but not necessarily indicative of mechanical instability. Another complication arises from a lack of robust topological signatures that can identify STZs from their parent liquidlike microstructure within a glassy matrix. There have been related efforts based upon the machine-learning-rooted concept of “structural” softness but with very limited predictive capabilities in terms of glass failure and deformation [31–33]. More focused studies of metallic glasses made an attempt to associate soft spots to the presence/absence of geometrically disfavored motifs and/or short/medium range ordering [34–36] but these local motifs on their own often fail to describe the collective nature of plasticity and shear banding in a broader context of amorphous plasticity. Our study aims to augment such efforts, directed mainly towards the notion of structural heterogeneity, by adding the elastic heterogeneity picture to the scene which is more conforming with the long-established notion of structure-property correlations in (metallic) glasses.

II. SIMULATIONS AND PROTOCOLS

Details of the molecular dynamics simulations are given in the Supplemental Material (SM) [37] (see also Refs. [38–44] therein) including relevant units, preparation protocols (Fig. S1), interatomic forces, and deformation parameters of FeNi, CoNiFe, CoNiCrFe, CoCrFeMn, CoNiCrFeMn, and $\text{Co}_5\text{Cr}_2\text{Fe}_{40}\text{Mn}_{27}\text{Ni}_{26}$ model metallic glasses [4]. In order to compute the elasticity tensor locally for simulated glasses, simple shear tests were performed on the xy plane at a fixed strain rate $\dot{\gamma}_{xy} = 10^{-5} \text{ ps}^{-1}$ and temperature $T = 300 \text{ K}$ up to a prescribed (pre)strain $\gamma_{xy} \leq 0.2$. In line with Refs. [45,46], we subsequently perturbed the simulation cell through six deformation modes in Cartesian directions xyz and evaluated resulting differences in atomwise stresses to construct the local elasticity tensor for each atom (see the SM). Relevant atom-based quantities were interpolated on a fine cubic grid to be used as input for our three-dimensional cluster processing. This methodology allows us to probe the spatial-dynamical

evolution of the local shear modulus $\mu = c_{xyxy}$ and associated percolation features near the failure transition in sheared glasses. We further measure the softening modulus h_{\min} defined as the maximum rate of the macroscopic stress drop for all the different compositions. The stress drop, typically defined as the difference between the overshoot stress and the subsequent flow stress, is associated with the initiation of a catastrophic shear band and has been used as an appropriate order parameter in model glass studies [47,48] showing meaningful variations with glass compositions and processing parameters [11]. We note that in metallic glass simulations and/or experiments a robust measurement of the macroscopic drop is not always feasible due to the lack of a well-defined steady flow regime that is expected to follow the stress overshoot. In a recent work [4], we established h_{\min} as a more robust experimentally relevant indicator of shear banding and associated structural features. Here, we show that the variations in h_{\min} tend to correlate with the softness properties as inferred from local elasticity.

III. RESULTS

Figure 1 displays results of the shear tests performed on the quenched CoNiFe and CoNiCrFe glasses. The cluster maps based on unstable regions with $\mu \leq 0$ are visualized in Figs. 1(b) and 1(c). Negative- μ clusters in Figs. S3(e)–S3(h) tend to form percolating networks on approach to failure that somewhat correlate with the mean-squared nonaffine displacements D_{\min}^2 maps (see SM for further details) illustrated in Figs. S3(a)–S3(d). We denote the fraction of unstable sites by (probability) p which appears to evolve in a nonmonotonic fashion [Figs. S5(b) and S5(c)], with a peak value p_{\max} that almost coincides with that of the (bulk) shear stress σ_{xy} (at $\gamma_{xy} \simeq 0.1$) as in Fig. 1(a). Apart from variations in p_{\max} , Figs. S5(a)–S5(f) show similar trends for the evolution of p with γ_{xy} corresponding to the other compositions. We notice $p > 0$ even in unstrained quenched glasses (at $\gamma_{xy} = 0$) owing to the distributed (but disconnected) networks of soft (Eshelby-like [49]) inclusions within the glassy matrix. We further note that p is controlled by statistical distributions of local shear modulus below the threshold (i.e., $\mu < 0$) showing a continuous reduction in the corresponding mean value and a gradual growth in the distribution width, as in Fig. S4, on approach to failure.

The above elasticity maps give a visual impression that the glass failure (at $\lambda_{\max} \simeq 0.1$) might indeed coincide with a percolation transition of softness at p_{\max} upon shear loading. In order to validate this picture, we adopted ideas from the classical percolation theory [50] including investigations of cluster sizes and their dynamical evolution. As a basic statistical property, n_s denotes the probability distribution function associated with the number of clusters containing s unstable sites. Figures 2(a) and 2(c) plot n_s associated with the CoNiFe and CoNiCrFe glasses at three different strains. The cluster size distributions tend to develop fairly long tails as p approaches p_{\max} . Our data suggest a robust power-law decay $n_s \propto s^{-\tau}$ with $\tau = 2.0$ and 2.1, associated with CoNiFe and CoNiCrFe, over at least two decades in s . The estimated range of exponent τ is fairly robust showing minimal compositional dependence (as reported in Table I) and/or variations near

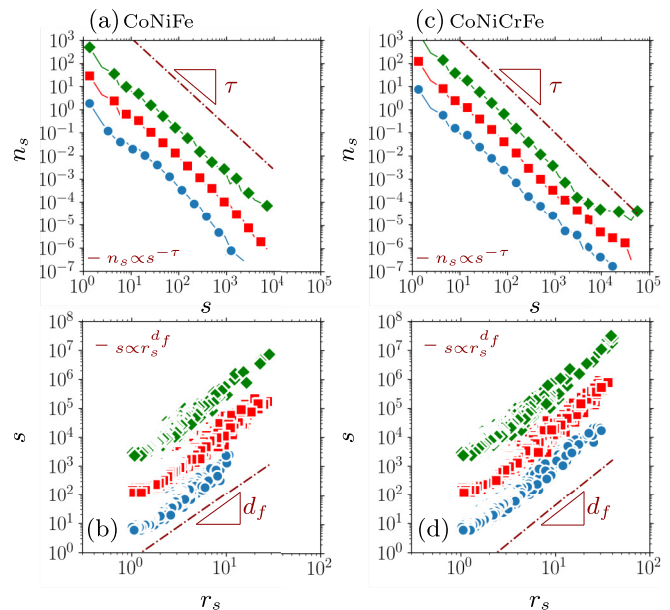


FIG. 2. Cluster size statistics corresponding to the CoNiFe and CoNiCrFe glasses. (a), (c) Cluster size distribution n_s . (b), (d) Scatter plot of cluster size s and associated radius of gyration r_s at different strains $\gamma_{xy} = 0.03$ (\bullet), 0.07 (\blacksquare), 0.1 (\blacklozenge). The dashed-dotted lines denote power laws $n_s \propto s^{-\tau}$ with (a) $\tau = 2.0$, (c) $\tau = 2.1$, and $s \propto r_s^{d_f}$ with (b) $d_f = 2.3$, (d) $d_f = 2.6$.

p_{\max} . The radius of gyration associated with a cluster of size s may be defined as $r_s^2 = \sum_{i=1}^s |\vec{r}_i - \vec{r}_0|^2 / s$ with the center of mass $\vec{r}_0 = \sum_{i=1}^s \vec{r}_i / s$. Figures 2(b) and 2(d) illustrate that $s \propto r_s^{d_f}$ with fractal dimension $d_f = 2.3$ and 2.6 corresponding to CoNiFe and CoNiCrFe, respectively. This almost agrees with Figs. 1(b) and 1(c) in that the soft spots tend to form fairly compact clusters in the latter glass whereas the former one is associated with more localized (but still system-spanning) features.

Figures 3(a) and 3(c) display the mean cluster size $S = \sum_s n_s s^2 / \sum_s n_s s$ and its evolution with p . The average size reveals a certain algebraic divergence of S on approach to the maximum fraction $p \rightarrow p_{\max}$. This divergence is demonstrated in Figs. 3(b) and 3(d) with the mean size scaling as $S \propto (p_{\max} - p)^{-\gamma}$ and $\gamma = 2.89$ and 2.20 corresponding to the CoNiFe and CoNiCrFe compositions, respectively. The proposed scaling is valid for a little less than a decade in $1 - p/p_{\max}$ down to a roll-off at small arguments potentially due to finite-size effects. The (squared) correlation length $\xi^2 = 2 \sum_s r_s^2 s^2 n_s / \sum_s s^2 n_s$ is defined based on a weighted average associated with the radius of gyration $r_s^2 = \sum_{i=1}^s |\vec{r}_i - \vec{r}_0|^2 / s$ of a cluster of size s , as shown in Figs. 4(a) and 4(c). Here, the center of mass is $\vec{r}_0 = \sum_{i=1}^s \vec{r}_i / s$. As p increases toward p_{\max} in Figs. 4(b) and 4(d), the correlation length scales as $\xi \propto (p_{\max} - p)^{-\nu}$ with $\nu = 1.26$ corresponding to CoNiFe and $\nu = 0.51$ for CoNiCrFe. The center and right panels of Fig. S5 show the mean cluster size S and correlation length ξ as a function of applied strain γ_{xy} associated with different compositions.

We repeated the above analysis to infer critical exponents corresponding to the other chemical compositions (see

TABLE I. Comparison between estimated scaling exponents associated with different chemical compositions and three-dimensional ($d = 3$) percolation theory.

Chemical composition	Cluster size distribution $n_s \propto s^{-\tau}$ τ	Mean cluster size $S \propto (p - p_{\max})^{-\gamma}$ γ	Correlation length $\xi \propto (p - p_{\max})^{-\nu}$ ν	Fractal dimension $s \propto r_s^{d_f}$ d_f
FeNi	1.96	2.23	0.87	2.27
CoNiFe	1.98	2.89	1.26	2.25
CoNiCrFe	2.05	2.20	0.51	2.62
CoCrFeMn	2.02	2.42	0.95	2.48
CoNiCrFeMn	2.00	2.26	0.62	2.43
Co ₅ Cr ₂ Fe ₄₀ Mn ₂₇ Ni ₂₆	1.93	2.69	0.94	2.28
CuZr [24]			0.85 ± 0.1	2.0
Percolation ($d = 3$) [50]	2.18	1.80	0.88	2.53
Directed percolation ($d = 3$) [51]		1.25	0.6	2.0

Fig. S6 and Table I) and sought for potential connections with the softening modulus h_{\min} . Figure 5 plots the latter and estimated critical exponents τ , γ , ν , and d_f for the FeNi, CoNiFe, CoNiCrFe, CoCrFeMn, CoNiCrFeMn, and Co₅Cr₂Fe₄₀Mn₂₇Ni₂₆ metallic glasses. As previously discussed, the cluster size exponent τ in Fig. 5(a) shows insignificant variations with chemical compositions. The scatter plot of h_{\min} and mean cluster size exponent γ in Fig. 5(b) suggests noticeable anticorrelations between the two observables. Likewise, the correlation length exponent ν seems to be

statistically (anti)correlated with h_{\min} as in Fig. 5(c). The increasing trend in the fractal dimension d_f might be indicative of localized (system-spanning) soft spots in good glasses that become increasingly packed in space as compositional variations lead to a smoother yielding transition. Given that there are only two independent exponents in standard percolation theory, the behavior of ν and γ should be largely controlled by variabilities in d_f . In Fig. S7, we present a robustness analysis of the scaling exponents with respect to variations in the local threshold.

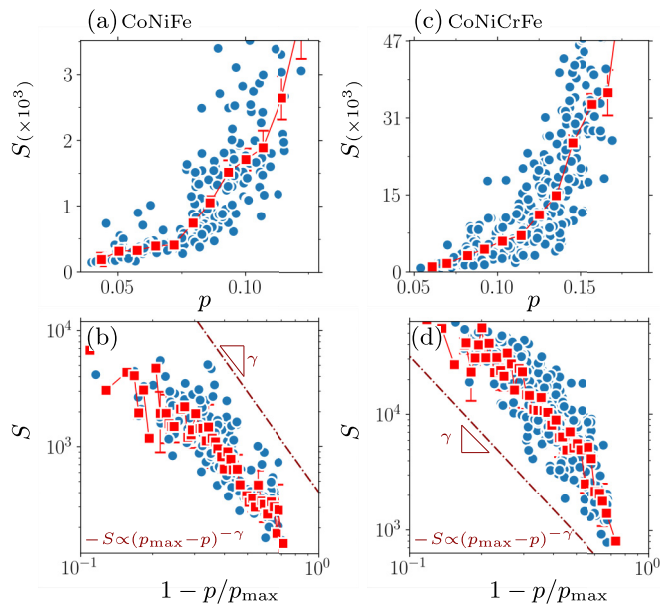


FIG. 3. Mean cluster size S plotted against p associated with the (a) CoNiFe and (c) CoNiCrFe glasses. The graphs in (b) and (d) are the same as (a) and (c) but plot S as a function of $1 - p/p_{\max}$ with (a) $p_{\max} = 0.14$ and (c) $p_{\max} = 0.20$. The (red) curves indicate binning averaged data. The dashed-dotted lines denote power laws $S \propto (p_{\max} - p)^{-\gamma}$ with (b) $\gamma = 2.89$ and (d) $\gamma = 2.20$.

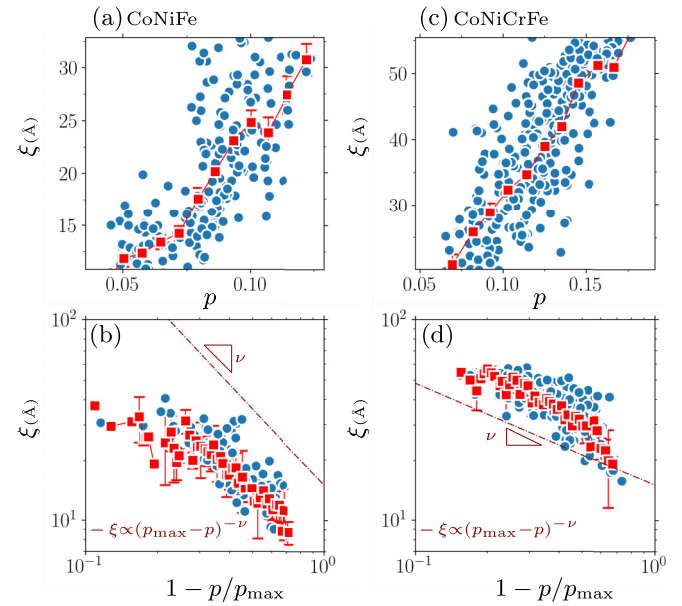


FIG. 4. Correlation length ξ plotted against p corresponding to the (a) CoNiFe and (c) CoNiCrFe glasses. The graphs in (b) and (d) are the same as (a) and (c) but plot ξ as a function of $1 - p/p_{\max}$ with (a) $p_{\max} = 0.14$ and (c) $p_{\max} = 0.20$. The (red) curves indicate binning averaged data. The dashed-dotted lines denote power laws $\xi \propto (p_{\max} - p)^{-\nu}$ with (b) $\nu = 1.26$ and (d) $\nu = 0.51$.

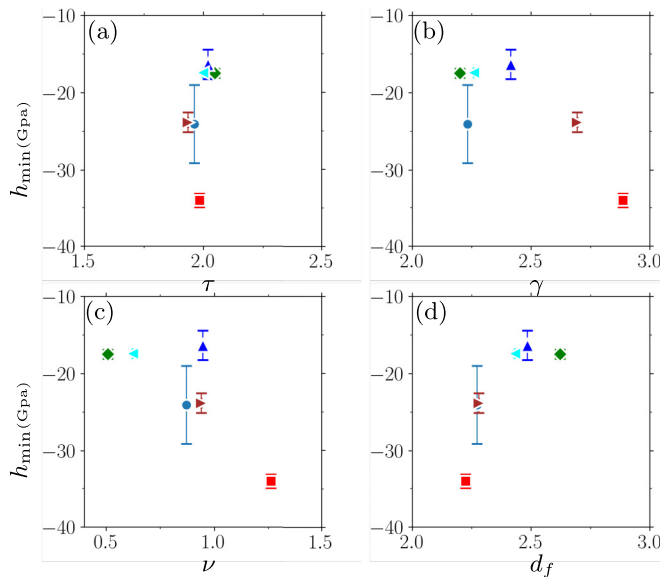


FIG. 5. Scatter plot of softening modulus h_{\min} and scaling exponents (a) γ (b) ν corresponding to the FeNi (●), CoNiFe (■), CoNiCrFe (◆), CoCrFeMn (▲), CoNiCrFeMn (◄), and Co₅Cr₂Fe₄₀Mn₂₇Ni₂₆ (◄) bulk metallic glasses.

IV. CONCLUSIONS AND DISCUSSIONS

We have presented direct evidence that the yielding transition of bulk metallic glasses is accompanied with a percolation threshold of softness upon failure across different chemical compositions. The former has been quantified by the softening modulus h_{\min} , indicative of the sharpness of the plastic yielding transition, and the latter was characterized by analyzing connected networks of mechanically soft regions that grow under application of external stress. Our analysis further indicates critical scaling features associated with the dynamics and the topology of soft clusters suggesting a close relevance of the percolation transition. Relevant scaling exponents and potential correlations with the macroscopic stress-strain curve have been considered from the compositional-dependence perspective. Table I features the range of estimated exponents corresponding to different multicomponent metallic glasses probed in this work and the study by Schall *et al.* [24] as well as those inferred from the percolation theory. In this framework, we find a fairly robust range (across different systems) associated with the cluster size exponent $1.9 \leq \tau \leq 2.1$ and comparable with theoretical predictions [50]. On the other hand, γ , ν , and d_f , inferred from the scaling of the correlation lengths and mean cluster sizes, somewhat correlate with softening modulus h_{\min} , suggesting that the softness percolation might influence macroscopic yielding properties through

compositional dependence. Such correlations may also suggest that the notion of universality in deformation and flow properties of multicomponent glasses could be limited owing to compositional/microstructural associations. Nevertheless, given a relatively narrow range of the softness exponents across different glasses, one might still consider the same universality class for the observed transition despite the fact that our results show substantial composition-based variabilities in yielding properties.

The present study brings different insights about (i) the microstructure-property paradigm in designing ductile multicomponents bulk metallic glasses, and (ii) the notion of elastic heterogeneity as a robust micromechanical indicator of plasticity. Along the lines of (i), the percolation of local elasticity upon failure and its precursory nature connects directly with the previous percolation studies. We, however, have revisited this concept within the framework of composition dependence of yielding transition and probed its meaningful variations/correlations with softness percolation. As for (ii), our work complements ongoing efforts within the glass community that aim to predict plasticity based on the notion of nonaffinity. Such predictions, mainly centered on structural/topological signatures of failure precursors, can be substantially improved by bringing micromechanical aspects (e.g., elastic heterogeneity) into the picture.

Our work has mainly focused on composition-dependent ductility and its correlations with softness percolation. Such correlations are potentially analogous to the preparation effects (i.e., quenching versus annealing) on the nature of the yielding transition. It is well established that slow cooling rates (i.e., annealing/aging) and associated structural relaxation leads to the annihilation of soft liquidlike spots (i.e., STZs) and therefore more brittle glasses [6]. Fast quench rates, on the other hand, tend to further amorphize (or rejuvenate) the glassy structure culminating in denser populations of STZs and thus enhanced ductility and (fracture) toughness. The investigation of the annealing protocol and its effects on softness-yielding correlations, as evidenced in Fig. 5, is an interesting topic that could be reserved as future work.

ACKNOWLEDGMENTS

This research was funded by the European Union Horizon 2020 research and innovation program under Grant Agreement No. 857470 and from the European Regional Development Fund via Foundation for Polish Science International Research Agenda PLUS program Grant No. MAB PLUS/2018/8. We wish to thank A. Esfandiarpour and R. Alvarez for providing the data sets.

- [1] L. Dai and Y. Bai, Basic mechanical behaviors and mechanics of shear banding in BMGs, *Int. J. Impact Eng.* **35**, 704 (2008).
- [2] C. A. Schuh, T. C. Hufnagel, and U. Ramamurty, Mechanical behavior of amorphous alloys, *Acta Mater.* **55**, 4067 (2007).
- [3] H. Ding and K. Yao, High entropy Ti₂₀Zr₂₀Cu₂₀Ni₂₀Be₂₀ bulk metallic glass, *J. Non-Cryst. Solids* **364**, 9 (2013).

- [4] K. Karimi, A. Esfandiarpour, R. Alvarez-Donado, M. J. Alava, and S. Papanikolaou, Shear banding instability in multicomponent metallic glasses: Interplay of composition and short-range order, *Phys. Rev. B* **105**, 094117 (2022).
- [5] D. V. Denisov, K. A. Lőrincz, W. J. Wright, T. C. Hufnagel, A. Nawano, X. Gu, J. T. Uhl, K. A. Dahmen, and P. Schall,

- Universal slip dynamics in metallic glasses and granular matter—linking frictional weakening with inertial effects, *Sci. Rep.* **7**, 43376 (2017).
- [6] Y. Cheng and E. Ma, Atomic-level structure and structure–property relationship in metallic glasses, *Prog. Mater. Sci.* **56**, 379 (2011).
- [7] Y. Cheng, A. Cao, and E. Ma, Correlation between the elastic modulus and the intrinsic plastic behavior of metallic glasses: The roles of atomic configuration and alloy composition, *Acta Mater.* **57**, 3253 (2009).
- [8] N. Wang, J. Ding, F. Yan, M. Asta, R. O. Ritchie, and L. Li, Spatial correlation of elastic heterogeneity tunes the deformation behavior of metallic glasses, *npj Comput. Mater.* **4**, 19 (2018).
- [9] F.-F. Wu, Z.-F. Zhang, and S. X.-Y. Mao, Transition of failure mode and enhanced plastic deformation of metallic glass by multiaxial confinement, *Adv. Eng. Mater.* **11**, 898 (2009).
- [10] M. Chen, A. Inoue, W. Zhang, and T. Sakurai, Extraordinary Plasticity of Ductile Bulk Metallic Glasses, *Phys. Rev. Lett.* **96**, 245502 (2006).
- [11] Y. Cheng, A. J. Cao, H. Sheng, and E. Ma, Local order influences initiation of plastic flow in metallic glass: Effects of alloy composition and sample cooling history, *Acta Mater.* **56**, 5263 (2008).
- [12] Y. Shi and M. L. Falk, Strain Localization and Percolation of Stable Structure in Amorphous Solids, *Phys. Rev. Lett.* **95**, 095502 (2005).
- [13] F. Albano and M. L. Falk, Shear softening and structure in a simulated three-dimensional binary glass, *J. Chem. Phys.* **122**, 154508 (2005).
- [14] N. Wang, Multi-scale modeling of spatial heterogeneity effect on the shear banding behaviors in metallic glasses, Ph.D. thesis, The University of Alabama, 2018.
- [15] J. C. Phillips and M. Thorpe, Constraint theory, vector percolation and glass formation, *Solid State Commun.* **53**, 699 (1985).
- [16] R. W. Hall and P. G. Wolynes, Microscopic Theory of Network Glasses, *Phys. Rev. Lett.* **90**, 085505 (2003).
- [17] S. G. Mayr, Relaxation kinetics and mechanical stability of metallic glasses and supercooled melts, *Phys. Rev. B* **79**, 060201(R) (2009).
- [18] A. J. Liu and S. R. Nagel, The jamming transition and the marginally jammed solid, *Annu. Rev. Condens. Matter Phys.* **1**, 347 (2010).
- [19] A. J. Liu, S. R. Nagel, W. Van Saarloos, and M. Wyart, The jamming scenario—an introduction and outlook, in *Dynamical Heterogeneities in Glasses, Colloids, and Granular Media* (Oxford University Press, New York, 2011), p. 298.
- [20] G. Düring, E. Lerner, and M. Wyart, Phonon gap and localization lengths in floppy materials, *Soft Matter* **9**, 146 (2013).
- [21] M. Wyart and M. E. Cates, Discontinuous Shear Thickening without Inertia in Dense Non-Brownian Suspensions, *Phys. Rev. Lett.* **112**, 098302 (2014).
- [22] K. H. Nagamanasa, S. Gokhale, A. Sood, and R. Ganapathy, Direct evidence for an absorbing phase transition governing yielding of a soft glass, [arXiv:1402.2730](https://arxiv.org/abs/1402.2730).
- [23] G. P. Shrivastav, P. Chaudhuri, and J. Horbach, Yielding of glass under shear: A directed percolation transition precedes shear-band formation, *Phys. Rev. E* **94**, 042605 (2016).
- [24] A. Ghosh, Z. Budrikis, V. Chikkadi, A. L. Sellerio, S. Zapperi, and P. Schall, Direct Observation of Percolation in the Yielding Transition of Colloidal Glasses, *Phys. Rev. Lett.* **118**, 148001 (2017).
- [25] P. Schall, D. A. Weitz, and F. Spaepen, Structural rearrangements that govern flow in colloidal glasses, *Science* **318**, 1895 (2007).
- [26] P. Cao, M. P. Short, and S. Yip, Potential energy landscape activations governing plastic flows in glass rheology, *Proc. Natl. Acad. Sci. U.S.A.* **116**, 18790 (2019).
- [27] S. Pauly, G. Liu, G. Wang, U. Kühn, N. Mattern, and J. Eckert, Microstructural heterogeneities governing the deformation of $\text{Cu}_{47.5}\text{Zr}_{47.5}\text{Al}_5$ bulk metallic glass composites, *Acta Mater.* **57**, 5445 (2009).
- [28] Z. Liu, R. Li, G. Liu, W. Su, H. Wang, Y. Li, M. Shi, X. Luo, G. Wu, and T. Zhang, Microstructural tailoring and improvement of mechanical properties in CuZr-based bulk metallic glass composites, *Acta Mater.* **60**, 3128 (2012).
- [29] Y. Zhang, Y. J. Zhou, J. P. Lin, G. L. Chen, and P. K. Liaw, Solid-solution phase formation rules for multi-component alloys, *Adv. Eng. Mater.* **10**, 534 (2008).
- [30] D. Richard, M. Ozawa, S. Patinet, E. Stanifer, B. Shang, S. A. Ridout, B. Xu, G. Zhang, P. K. Morse, J.-L. Barrat, L. Berthier, M. L. Falk, P. Guan, A. J. Liu, K. Martens, S. Sastry, D. Vandembroucq, E. Lerner, and M. L. Manning, Predicting plasticity in disordered solids from structural indicators, *Phys. Rev. Mater.* **4**, 113609 (2020).
- [31] E. D. Cubuk, S. S. Schoenholz, J. M. Rieser, B. D. Malone, J. Rottler, D. J. Durian, E. Kaxiras, and A. J. Liu, Identifying Structural Flow Defects in Disordered Solids Using Machine-Learning Methods, *Phys. Rev. Lett.* **114**, 108001 (2015).
- [32] Z. Fan, J. Ding, and E. Ma, Machine learning bridges local static structure with multiple properties in metallic glasses, *Mater. Today* **40**, 48 (2020).
- [33] E. Boattini, S. Marín-Aguilar, S. Mitra, G. Foffi, F. Smallenburg, and L. Filion, Autonomously revealing hidden local structures in supercooled liquids, *Nat. Commun.* **11**, 5479 (2020).
- [34] J. Ding, S. Patinet, M. L. Falk, Y. Cheng, and E. Ma, Soft spots and their structural signature in a metallic glass, *Proc. Natl. Acad. Sci. U.S.A.* **111**, 14052 (2014).
- [35] J. Ding, Y.-Q. Cheng, and E. Ma, Full icosahedra dominate local order in $\text{Cu}_{64}\text{Zr}_{34}$ metallic glass and supercooled liquid, *Acta Mater.* **69**, 343 (2014).
- [36] J. Ding, Y.-Q. Cheng, H. Sheng, M. Asta, R. O. Ritchie, and E. Ma, Universal structural parameter to quantitatively predict metallic glass properties, *Nat. Commun.* **7**, 13733 (2016).
- [37] See Supplemental Material at <http://link.aps.org/supplemental/10.1103/PhysRevMaterials.7.063601> for further discussions relevant to simulation details.
- [38] S. Plimpton, Fast parallel algorithms for short-range molecular dynamics, *J. Comput. Phys.* **117**, 1 (1995).
- [39] M. W. Glasscott, A. D. Pendergast, S. Goines, A. R. Bishop, A. T. Hoang, C. Renault, and J. E. Dick, Electrosynthesis of high-entropy metallic glass nanoparticles for designer, multi-functional electrocatalysis, *Nat. Commun.* **10**, 2650 (2019).
- [40] R. Alvarez-Donado, S. Papanikolaou, A. Esfandiarpour, and M. J. Alava, Viewing high entropy alloys through glasses:

- Linkages between solid solution and glass phases in multicomponent alloys, *Phys. Rev. Mater.* **7**, 025603 (2023).
- [41] C. Alcock, O. Kubaschewski, and P. Spencer, *Materials Thermochemistry* (Pergamon Press, Oxford, UK, 1993).
- [42] W.-M. Choi, Y. H. Jo, S. S. Sohn, S. Lee, and B.-J. Lee, Understanding the physical metallurgy of the CoCrFeMnNi high-entropy alloy: an atomistic simulation study, *npj Comput. Mater.* **4**, 1 (2018).
- [43] A. Lees and S. Edwards, The computer study of transport processes under extreme conditions, *J. Phys. C* **5**, 1921 (1972).
- [44] M. L. Falk and J. S. Langer, Dynamics of viscoplastic deformation in amorphous solids, *Phys. Rev. E* **57**, 7192 (1998).
- [45] H. Mizuno, S. Mossa, and J.-L. Barrat, Measuring spatial distribution of the local elastic modulus in glasses, *Phys. Rev. E* **87**, 042306 (2013).
- [46] M. Tsamados, A. Tanguy, C. Goldenberg, and J.-L. Barrat, Local elasticity map and plasticity in a model Lennard-Jones glass, *Phys. Rev. E* **80**, 026112 (2009).
- [47] M. Ozawa, L. Berthier, G. Biroli, A. Rosso, and G. Tarjus, Random critical point separates brittle and ductile yielding transitions in amorphous materials, *Proc. Natl. Acad. Sci. U.S.A.* **115**, 6656 (2018).
- [48] K. Chen and K. S. Schweizer, Theory of yielding, strain softening, and steady plastic flow in polymer glasses under constant strain rate deformation, *Macromolecules* **44**, 3988 (2011).
- [49] J. D. Eshelby, The elastic field outside an ellipsoidal inclusion, *Proc. R. Soc. London, Ser. A* **252**, 561 (1959).
- [50] D. Stauffer and A. Aharony, *Introduction to Percolation Theory* (Taylor & Francis, London, 2018).
- [51] H. Hinrichsen, Non-equilibrium critical phenomena and phase transitions into absorbing states, *Adv. Phys.* **49**, 815 (2000).